Unravelling the Growth of Supramolecular Metal–Organic Frameworks Based on Metal–Nucleobase Entities

ARTICLE *in* CRYSTAL GROWTH & DESIGN · JANUARY 2015

Impact Factor: 4.89 · DOI: 10.1021/cg501804h

CRYSTAL GROWTH & DESIGN

Article

pubs.acs.org/crystal

Unravelling the Growth of Supramolecular Metal–Organic Frameworks Based on Metal-Nucleobase Entities

Jintha Thomas-Gipson,‡ Rubén Pérez-Aguirre,‡ Garikoitz Beobide, Oscar Castillo,* Antonio Luque, Sonia Pérez-Yáñez,* and Pascual Román

Departamento de Química Inorgánica, Facultad de Ciencia y Tecnología, Universidad del País Vasco (UPV/EHU), Apartado 644, E–48080 Bilbao, Spain

Supporting Information

ABSTRACT: The present work provides the basis to obtain three-dimensional (3D) extended porous supramolecular assemblies named supramolecular metal–organic frameworks (SMOFs). This goal can be achieved by considering three key factors: (i) the use of rigid building units, (ii) the establishment of predictable and rigid synthons between the building units, and (iii) the non-coplanarity of functional groups involved in the predictable synthons. Throughout this report we demonstrate the suitability of this synthetic strategy supported by six new SMOFs based on metal-nucleobase entities which fulfill the stated requirements: $[Co(ThioG)_3]$ (**SMOF-4**; ThioG = thioguaninato), $[Co(Hade)_2X_2]$ (**SMOF-5**, **SMOF-6**; Hade = adenine and X = Cl^-, Br^-), $[Cu_8(\mu_3\text{-}OH)_4(\mu_4\text{-}OH)_4(ade)_4(\mu\text{-}ade)_4(\mu\text{-}Hade)_2]$ (**SMOF-7**; ade = adeninato), $[Cu_4(\mu_3\text{-}ade)_4(\mu\text{-}ade)_2(pentylNH_2)_2(CH_3OH)_2(CO_3)_2(H_2O)_2]$ (**SMOF-8**; $pentylNH_2$ = 1-pentylamine), and $[Cu_2(\mu\text{-}ade)_2(ade)(\mu\text{-}OH)(H_2O)(CH_3OH)]_n$ (**SMOF-9**). **SMOF-4** is built up from monomeric entities in which bidentate thioguaninato ligands establish complementary hydrogen bonding interactions in non-coplanar directions leading to supramolecular layers that are further connected resulting in a porous structure with one-dimensional (1D) channels. The hydrogen bonding interactions among Watson–Crick and sugar edges of monomeric entities in **SMOF-5** give rise to a triply interpenetrated supramolecular framework. Octameric clusters in **SMOF-7** are self-assembled by hydrogen bonding to yield a porous 3D network. **SMOF-8** is built up from tetranuclear units that are linked via base pairing interactions involving Watson–Crick faces to afford layers whose assembly generates a two-dimensional pore system. **SMOF-9** is in between pure MOFs and SMOFs since it consists of 1D infinite coordination polymers held together by complementary hydrogen bonding interactions into a 3D supramolecular porous structure.

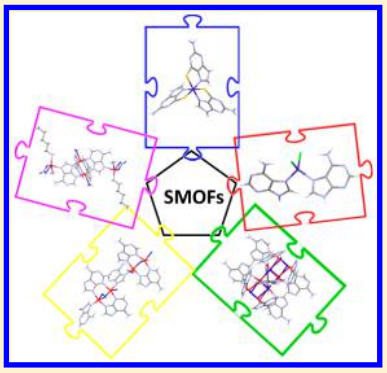

INTRODUCTION

Metal–organic frameworks (MOFs) encompass an area of chemistry that has experienced impressive growth during the last decades because of their various potential applications in catalysis, gas storage, chemical separations, sensing, ion exchange, drug delivery, and optics.[1] Regarding the adsorption field, it is worth mentioning that their large surface areas, adjustable pore sizes, and controllable functionalities are key factors that make MOFs promising candidates for adsorptive separations and purification purposes.[2,3] Taking into account the great potential of MOFs, we decided to explore a related type of material, in which the coordination bonds are replaced with hydrogen bonds as connectors, which are also directional and predictable interactions, to sustain the three-dimensional (3D) crystal building containing potentially accessible voids (Figure 1).[4,5] Although such kinds of alternative materials can arise a similar fascination to that of MOFs, the crystal engineering principles and the synthetic approach are not yet settled, and examples of this kind of material are rather scarce. In this sense a first clue to reach this goal can be inferred using the naive analogy of soft and rigid balls. Soft balls can adjust their shape to provide an efficient packing leaving almost no space in between. However, rigid balls do not have the option

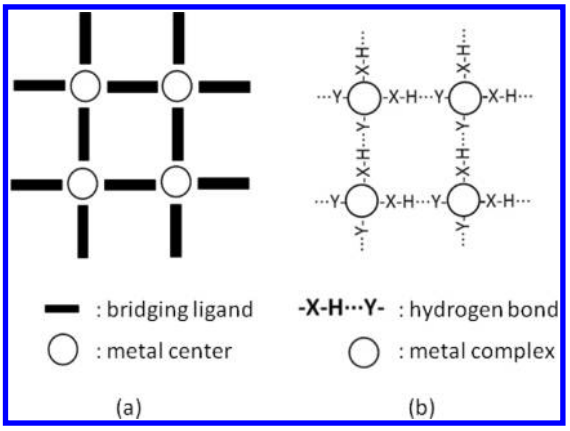

Figure 1. Similarity between (a) coordination bonds and (b) hydrogen bonding interactions as structure directing agents.

Received: December 10, 2014
Revised: January 7, 2015
Published: January 12, 2015

DOI: 10.1021/cg501804h
Cryst. Growth Des. 2015, 15, 975–983

of changing their shape, and, as a consequence, their packing is less effective giving rise to the presence of voids. In other words, flexible objects pack effectively, while rigid objects do not unless they present very specific and appropriate shape, such as cubes, triangular, rectangular and hexagonal prisms, etc.[6] This simple idea has helped us develop a synthetic strategy to obtain supramolecular metal−organic frameworks (SMOFs)[7,8] with potentially accessible voids as an alternative to more conventional metal−organic frameworks (MOFs).

The synthetic strategy is based on the following key factors: (i) the use of rigid building units, (ii) the establishment of predictable and rigid synthons between the building units, and (iii) the noncoplanarity of functional groups involved in the predictable synthons. The rigidity of the building units (discrete complexes) can be achieved using rigid ligands bonded through multiple positions. It means, in most common cases, a double anchoring of the ligand by means of two simultaneous coordination bonds or the combination of a coordination bond and an intramolecular hydrogen bond. The predictability and rigidity of the synthons require the presence of adjacent functional groups, incorporated into the rigid ligands, able to establish complementary hydrogen bonding interactions. Finally, the requisite of noncoplanar arrangement of the synthons comes from our objective of obtaining 3D extended systems that is achieved by the presence of at least three noncoplanar synthons. The use of nonplanar coordination geometries for the complexes makes this last condition easy to accomplish.

From previous studies we realized that a suitable system that would fulfill all of the above-described requirements for obtaining SMOFs are the discrete metal-nucleobase systems, especially those based on purine nucleobases.[9−11] These ligands provide, on the one hand, the advantage of increased rigidity of the supramolecular building block due to the coordination through multiple positions, and, on the other hand, they present many edges capable of establishing complementary hydrogen bonding interactions that provide rigid and predictable synthons (Scheme 1). Therefore, the adequate selection of the metal-nucleobase discrete entity that would afford a non-coplanar arrangement of the nucleobases could provide the desired supramolecular porous materials.

Scheme 1. Adenine Edges Capable of Establishing Rigid Complementary Double Hydrogen Bonding Synthons

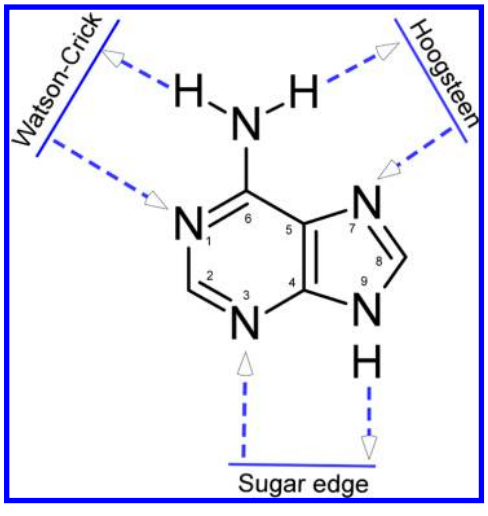

The preliminary results were achieved employing $[Cu_2(\mu\text{-adenine})_4(X)_2]^{2+}$ (**SMOF-1** and **SMOF-2**; X = Cl^-, Br^-) as supramolecular building blocks in which two or more nucleobases are tightly anchored to the metal centers by two donor positions (N3 and N9 sites), imposing a rigid building unit.[7,12] Moreover, this coordination motif imposes a rigid geometrical restraint among the nucleobases providing a set of noncoplanar synthons that otherwise would be very difficult to achieve. As many hydrogen donor/acceptor positions of the nucleobase remain free, these discrete entities are able to self-assemble among them by means of double hydrogen bonds to provide extended supramolecular solids in which great channels are present. These compounds present a surface instability that creates a diffusion barrier permeated only by strong interacting adsorbate molecules such as CO_2 but not N_2, H_2, and CH_4, which makes them attractive for selective gas adsorption and separation technologies. Zaworotko et al. reported an analogous compound, based on the $[Cu_2(\mu\text{-adenine})_4(X)_2]^{2+}$ dinuclear entity, replacing the halides by bulkier TiF_6^{2-} anions improving the chemical stability of the supramolecular network toward humidity, thus avoiding the surface instability, and therefore, being able to adsorb CO_2, CH_4, and N_2.[13] These studies also pointed out the relevance of the solvent selection because strong hydrogen bond donor and acceptor solvents such as water molecules could disrupt the direct hydrogen bonding interactions between the nucleobases that are the key factors to achieve this type of compound.

In this report we demonstrate the suitability of this synthetic strategy to afford the self-assembly of rigid mono- or polynuclear entities by means of a set of non-coplanar synthons into supramolecular porous materials.

EXPERIMENTAL SECTION

Synthesis of **SMOF-4**, $[Co(ThioG)_3]$. 0.59 mL (0.4 mmol) of pentylamine was added dropwise to 0.0685 g (0.4 mmol) of 6-thioguanine dissolved in 20 mL of water, and the mixture was stirred in an ice bath for 1 h. To this mixture was added a 10 mL solution of 0.0291 g (0.1 mmol) of $Co(NO_3)_2{\cdot}6H_2O$ dissolved in water. The brown-colored solution was then stirred for 2 h in an ice bath and then left for evaporation. Brown-colored single-crystals were separated after 2 weeks. The compound was also obtained on replacing $Co(NO_3)_2{\cdot}6H_2O$ with $CoSO_4{\cdot}7H_2O$. Yield: 60%. Anal. Calcd (found) for $C_{15}H_{12}CoN_{15}S_3{\cdot}6.7H_2O$: C, 26.56 (26.68); H, 3.78 (3.70); N, 30.98 (31.29), S, 14.18 (14.21), Co, 8.69 (8.75). Main IR features (cm^{-1}; KBr pellets): 3422s, 1611m, 1498w, 1459w, 1385m, 1306sh, 1243vs, 1190m, 1146s, 983s, 933w, 893w, 836w, 803w, 743w, 716w, 680w, 630w, 523w.

Synthesis of **SMOF-5**, $[Co(Hade)_2Cl_2]$. This compound was obtained as deep blue polycrystalline form by the dropwise addition of a propanolic solution of adenine (0.0270 g, 0.2 mmol) into a stirring solution of 0.0238 g of $CoCl_2{\cdot}6H_2O$ (0.1 mmol). When the synthesis was performed in methanol bad quality crystals were obtained. Then, single crystals of good quality were obtained by using diffusion techniques. Yield: precipitate 70%, crystals 50%. Anal. Calcd (found) for $C_{10}H_{10}Cl_2CoN_{10}$: C, 30.02 (30.09); H, 2.52 (2.47); N, 35.01 (34.93); Co, 14.73 (14.82) %. Main IR features (cm^{-1}; KBr pellets): 3391vs, 3258vs, 3133vs, 3058vs, 2346w, 2280w, 2186w, 2016w, 1943w, 1790w, 1696vs, 1611s, 1498m, 1459w, 1397s, 1327m, 1237m, 1171m, 1105w, 1066w, 1016w, 942m, 895m, 856w, 778m, 712m, 631w, 610m, 530m.

Synthesis of **SMOF-6**, $[Co(Hade)_2Br_2]$. The synthesis is the same as for **SMOF-5** but replacing $CoCl_2{\cdot}6H_2O$ by $CoBr_2$. Yield: precipitate 60%. All the attempts to grow single-crystals were unsuccessful. Anal. Calcd (found) for $C_{10}H_{10}Br_2CoN_{10}$: C, 24.56 (24.49); H, 2.06 (2.15); N, 28.64 (28.57); Co, 12.05 (12.01) %. Main IR features (cm^{-1}; KBr pellets): 3450s, 3341vs, 3066s, 2817w, 2671w, 2284w, 1951w, 1663vs,

DOI: 10.1021/cg501804h
Cryst. Growth Des. 2015, 15, 975−983

Table 1. Crystallographic Data and Structure Refinement Details[a]

	SMOF-4	SMOF-5	SMOF-7	SMOF-8	SMOF-9
formula	$C_{15}H_{12}CoN_{15}S_3$	$C_{10}H_{10}Cl_2CoN_{10}$	$C_{50}H_{50}Cu_8N_{50}O_8$	$C_{30.85}H_{46.80}Cu_{3.55}N_{21.55}O_{8.20}$	$C_{16}H_{19}Cu_2N_{15}O_3$
MW (g mol^{-1})	557.51	400.11	1987.72	1076.37	596.54
crystal system	trigonal	monoclinic	monoclinic	triclinic	monoclinic
space group	$P\bar{3}$	$C2/c$	$Ccca$	$P\bar{1}$	$C2/c$
a (Å)	16.7297(14)	11.2442(18)	20.1899(5)	12.646(5)	23.472(7)
b (Å)	16.7297(14)	6.9401(7)	28.964(2)	13.136(5)	16.398(3)
c (Å)	6.5245(4)	18.760(2)	16.5403(5)	13.158(5)	18.803(5)
α (deg)	90	90	90	73.784(5)	90
β (deg)	90	95.000(13)	90	81.840(5)	112.30(3)
γ (deg)	120	90	90	62.368(5)	90
V (Å^3)	1581.4(2)	1458.4(3)	9672.6(8)	1859.2(12)	6696(3)
Z	2	4	4	1	8
ρ_{calcd} (g cm^{-3})	1.171	1.822	1.365	0.961	1.184
μ (mm^{-1})	0.769	12.758	1.790	1.047	1.899
reflections collected	4690	5201	33482	6909	5529
unique data/parameters	2300/103	1462/109	5277/272	6909/269	5529/325
R_{int}	0.1278	0.0656	0.0630	0.1840	0.0972
goodness of fit (S)[b]	1.033	1.045	1.092	0.773	0.741
R_1[c]/wR_2[d] [all data]	0.0924/0.1673	0.0664/0.1606	0.0872/0.2221	0.2330/0.2882	0.1519/0.2091
R_1[c]/wR_2[d] [$I > 2\sigma(I)$]	0.0646/0.1585	0.0606/0.1560	0.0721/0.2115	0.1044/0.2691	0.0800/0.1840

[a]Reported data do not include the variable amount of solvent molecules present in the channels. [b]$S = [\sum w(F_0^2 - F_c^2)^2/(N_{obs} - N_{param})]^{1/2}$. [c]$R_1 = \sum||F_0| - |F_c||/\sum|F_0|$. [d]$wR_2 = [\sum w(F_0^2 - F_c^2)^2/\sum wF_0^2]^{1/2}$; $w = 1/[\sigma^2(F_0^2) + (aP)^2 + bP]$ where $P = (\max(F_0^2,0) + 2Fc^2)/3$ with $a = 0.0691$ (**1**), 0.0897 (**2**), 0.1440 (**3**), 0.1283 (**4**), 0.0584 (**5**) and $b = 4.8645$ (**2**), 1.6779 (**3**).

1596vs, 1513w, 1480s, 1416s, 1360w, 1343s, 1306s, 1246s, 1170w, 1120w, 1020w, 1063w, 1030w, 973m, 910m, 870w, 791m, 763m, 722s, 680w, 638m, 627m, 557s, 545m, 532s.

Synthesis of **SMOF-7**, $[Cu_8(\mu_3\text{-}OH)_4(\mu_4\text{-}OH)_4(ade)_4(\mu\text{-}ade)_4(\mu\text{-}Hade)_2]$. Twenty milliliters of an aqueous methanolic solution (1:1) containing adenine (0.8 mmol, 0.108 g) were added to 20 mL of an aqueous solution of $CuSO_4{\cdot}5H_2O$ (0.4 mmol, 0.0998 g) leading to a solution of pH = 3. Immediately a dark blue precipitate appeared. Then, sulfuric acid was added until complete dissolution of the precipitate (pH = 1.5). A glass vial with the resulting solution was placed in an Erlenmeyer flask containing triethylamine favoring the difussion of the base into the solution. A few days later a small amount of purple crystals appeared mixed with a major unknown phase.

Synthesis of **SMOF-8**, $[Cu_4(\mu_3\text{-}ade)_4(\mu\text{-}ade)_2(pentylNH_2)_2(CH_3OH)_2(CO_3)_2(H_2O)_2]$. Single crystals of this compound were obtained by adding a 10 mL methanolic solution of 0.0198 g of $Cu(OOCCH_3)_2{\cdot}H_2O$ (0.1 mmol) to a methanolic solution (20 mL) of 0.0206 g of adenine (0.15 mmol) mixed with 0.59 mL of pentylamine. The green-colored solution was stirred for 1 h and left evaporating at room temperature. On evaporating the color of the solution started changing to blue-violet. After 2 weeks, violet-colored prismatic shaped crystals appeared. The crystals are unstable out from the mother liquid.

Synthesis of **SMOF-9**, $[Cu_2(\mu\text{-}ade)_2(ade)(\mu\text{-}OH)(H_2O)(CH_3OH)]_n$. Single crystals of this compound were obtained by the slow addition of a 10 mL methanolic solution of 0.0199 g of $Cu(OOCCH_3)_2{\cdot}H_2O$ (0.1 mmol) into a methanolic solution (50 mL) of 0.0546 g of adenine (0.4 mmol) mixed with 0.59 mL of pentylamine. The green-colored solution was stirred for 1 h and left evaporating at room temperature. Few blue needle like crystals that correspond to **SMOF-9** appeared in a time period of 1 week, mixed with violet crystals of **SMOF-8**. Yield: 5%. Anal. Calcd (found) for $C_{16}H_{19}Cu_2N_{15}O_3{\cdot}8.5(CH_3OH)$: C, 33.87 (33.77); H, 6.15 (6.08); N, 24.18 (24.09); Cu, 14.63 (14.74) %. Main IR features (cm^{-1}; KBr pellets): 3446s, 3356vs, 3123s, 1671s, 1418m, 1398m, 1385m, 1333m, 1308s, 1268m, 1251w, 1191m, 1149m, 1123w, 1022w, 979w, 939m, 910w, 875w, 845w, 797m, 738w, 723s, 641m, 620w, 570w, 541m.

Physical Measurements. Elemental analyses (C, H, N, S) were performed on an Euro EA elemental analyzer, whereas the metal content was determined by inductively coupled plasma atomic emission spectrometer (ICP-AES) from Horiba Yobin Yvon Activa. The IR spectra (KBr pellets) were recorded on a FTIR 8400S Shimadzu spectrometer in the 4000−400 cm^{-1} spectral region. Dinitrogen (77 K) and carbon dioxide (273 K) physisorption data were recorded on activated samples (vacuum at 100 °C for 4 h) with a Quantachrome QUADRASORB-SI-MP and a Quantachrome Autosorb-iQ-MP, respectively. The specific surface area was calculated from the adsorption branch in the relative pressure interval from 0.01 to 0.10 using the Brunauer−Emmett−Teller (BET) method.

X-ray Diffraction Data Collection and Structure Determination. Single-crystal X-ray diffraction data were collected on an Oxford Diffraction Xcalibur diffractometer with graphite monochromated Mo Kα radiation ($\lambda = 0.71073$ Å) at 100(2) K for **SMOF-4** and **SMOF-7**, and at 293 K for **SMOF-8**, and on an Agilent Technologies SuperNova diffractometer with Cu Kα radiation (1.54185 Å) for **SMOF-5** and **SMOF-9**. Data reduction was done with the CrysAlisPro program.[14] All the structures were solved by direct methods using the SIR92 program[15] and refined by full-matrix least-squares on F^2 including all reflections (SHELXL97).[16] All calculations for these structures were performed using the WINGX crystallographic software package.[17] After the initial structure solution was completed, the difference Fourier map for **SMOF-4**, **-7**, **-8**, and **-9** showed the presence of substantial electron density at the voids of the crystal structure that was impossible to model. Therefore, its contribution was subtracted from the reflection data by the SQUEEZE method[18] as implemented in PLATON.[19] During the data reduction process it became clear that the crystal specimen of **SMOF-8** was a nonmerohedric twin with a twin law: (1.026 −0.077 0.038/0.070 0.963 0.012/−0.023 −0.000 1.003). The final result showed a percentage of twinned component of 24.3%. Additionally, one of the metal centers (Cu2) and its coordinated ligands present a partial occupation of 0.78. Relevant data adquisition and refinement parameters are gathered in Table 1. CCDC 1038651−1038655 contain the supplementary crystallographic data for this paper.

RESULTS AND DISCUSSION

Structural Description of $[Co(ThioG)_3]$ (SMOF-4). The basic media of the reaction favored the oxidation to Co(III), as ensured by its diamagnetic nature, giving rise to neutral monomeric $[Co(ThioG)_3]$ entities. Three thioguaninato

DOI: 10.1021/cg501804h
Cryst. Growth Des. 2015, 15, 975−983

ligands, in its 9*H*-tautomeric form, are coordinated in a bidentate chelating mode to the Co(III) atoms by their N7 and S6 atoms affording an octahedral coordination environment. Coordination bonds lengths and angles are gathered in the Supporting Information. The coordination mode of the nucleobase analogue renders a rigid metal-complex and, at the same time, exposes its Watson−Crick (N1, N2) and sugar edges (N3, N9) providing a set of non-coplanar synthons with dihedral angles of 87° (Figure 2a). Therefore, this discrete

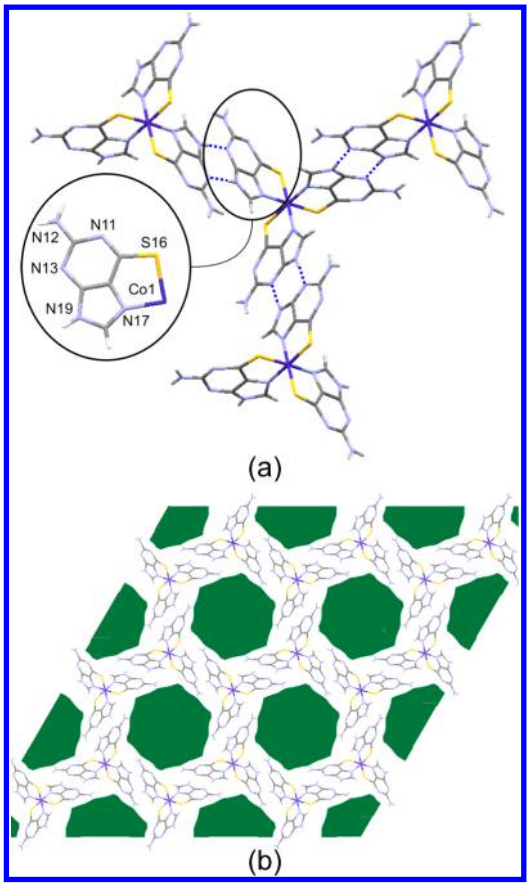

Figure 2. (a) Interactions among the monomeric entities and numbering scheme. (b) Projection of the crystal packing of **SMOF-4** along the crystallographic *c* axis. Green-colored regions represent the solvent accessible void.

complex entity fulfils the previously stated requirements for the success in obtaining a supramolecular porous material. In fact, there is a previous work based on similar discrete entities but using 6-thioguanosine that provides a complementary hydrogen bonding interaction involving only the Watson−Crick face (N1, N2) as the sugar edge is blocked by the sugar residue. It affords a supramolecular assembly containing great voids that are occupied by the sugar residue of the thioguanosine.[20] In **SMOF-4** both sides of the 6-thioguaninato are available to contribute to the supramolecular assembly. The sugar edge (N3, N9) of the nucleobases establishes a double hydrogen bonding interaction with the nucleobases of three neighboring entities to give a $R_2^2(8)$ ring (Table 2). This rigid synthon, based on direct thioguaninato···thioguaninato pairing interactions, leads to layers in the *ab* plane in which Δ and Λ isomers of the trischelate complex are sequentially arranged similarly to what happens in layered $[M(ox)_3]^{n-}$ based compounds.[21,22] The resulting arrangement corresponds to

Table 2. Structural Parameters (Å, °) of Noncovalent Interactions in SMOF-4[a]

Hydrogen Bonding Interactions					
D−H···A[b]		H···A	D···A	D−H···A	
N19−H19···N13[i]		2.03	2.875(5)	167	
N12−H12···S16[ii]		2.69	3.467(4)	151	
C18−H18···S16[iii]		2.67	3.415(4)	138	
$\pi-\pi$ Interactions[c]					
ring···ring[d]	angle	DC	α	DZ	DXY
h···h[iv]	0.0	3.46	18.5	3.28	1.10

[a]Symmetry codes: (i) $-x, -y + 1, -z + 2$; (ii) $x - y, x, -z + 1$; (iii) $-x + y, -x + 1, z + 1$; (iv) $-x, -y + 1, -z + 1$. [b]D: donor; A: acceptor. [c]Angle: dihedral angle between the planes (deg), DC: distance between the centroids of the rings (Å), α: angle between the normal to the first ring and the DC vector (deg), DZ: interplanar distance (Å), DXY: lateral displacement (Å). [d]h: hexagonal ring of the thioguanine.

the Shubnikov hexagonal **hcb** topology with a (6^3) point symbol.[23−25] The interactions among the three-connected uninodal two-dimensional (2D) nets are linked via weaker hydrogen bonds (N2−H···S6 and C8−H···S6) and reinforced with $\pi-\pi$ interactions, (Table 2) leading to an **acs** topology and $(4^9.6^6)$ point symbol that corresponds to a porous crystal structure with an estimated surface area of 887 m^2/g and 43% of void space based on theoretical calculations.[26,19] The resulting porous structure consists of one-dimensional (1D) channels that run along the crystallographic *c* axis with a diameter of 8.2−9.4 Å (Figure 2b). It is worth mentioning the template effect exerted by the pentylamine. This molecule provides the basic media that this reaction requires, and, at the same time, the tendency of the aliphatic tails to form aggregates in water promotes the growth of the supramolecular structure around them. In fact, the same synthesis but using different amines with shorter aliphatic tails does not provide this compound.

According to N_2 (77 K) and CO_2 (273 K) adsorption studies, this compound is highly selective toward CO_2 adsorption (Figure 3). The N_2 adsorption curve exhibits features of a nonporous material, and, accordingly, the fitting of the adsorption area to BET equation leads to a negligible value. However, it shows a significant CO_2 uptake with a non-saturating curve reaching a value of 1.4 mmol/g at 1 bar. This behavior has been described in the introduction section for

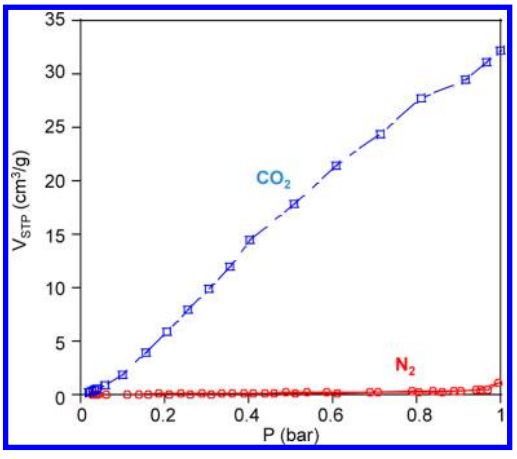

Figure 3. Adsorption isotherms for N_2 (77 K) and CO_2 (273 K), of a fresh sample of **SMOF-4**.

DOI: 10.1021/cg501804h
Cryst. Growth Des. 2015, 15, 975−983

SMOF-1 and **SMOF-2**, and its explanation for **SMOF-4** probably would also be related to a crystal surface instability.

Structural Description of $[Co(Hade)_2Cl_2]$ (SMOF-5). **SMOF-5** contains neutral monomeric $[Co(Hade)_2Cl_2]$ units. 9*H*-Adenine acts as a monodentate ligand, and it is coordinated to the Co(II) metal center through the N7 position that it is very usual for unsubstituted adenine moieties, but it requires a second anchoring position of the nucleobase to be stiff enough to meet our requirements. Such stiffness is achieved by the presence of intramolecular hydrogen bonding interactions between the amino hydrogen atom and the chloride one. The adenine also exposes its Watson−Crick and sugar-edges to establish intermolecular complementary hydrogen bonding interactions with adjacent adenine molecules (Figure 4a).

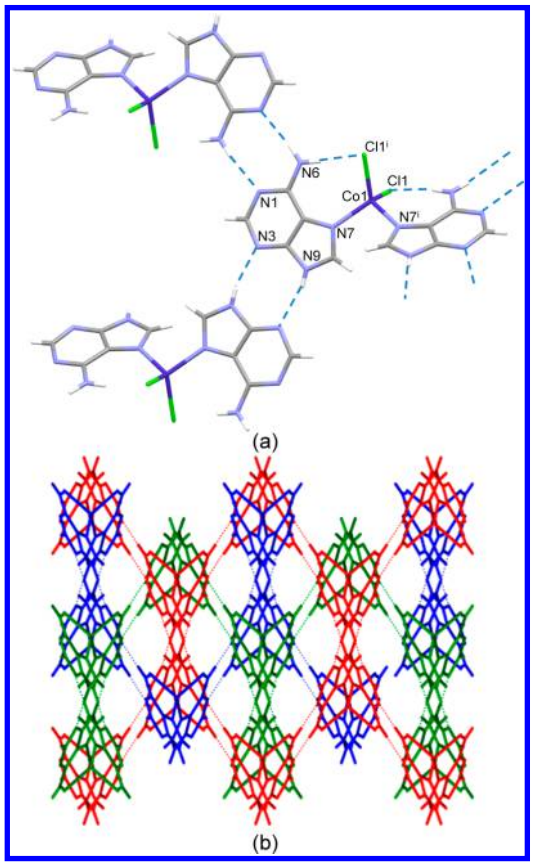

Figure 4. (a) Rigid synthon formed by direct supramolecular interactions in **SMOF-5**. (b) Triple interpenetrated crystal structure of **SMOF-5**. Each subnet is represented using a different color.

The rigid synthons involving WC···WC and sugar···sugar edges interactions give rise in both cases to $R_2^2(8)$ hydrogen bonding rings, that are well-known structural synthons between self-assembling adenine fragments.[27−33] These interactions build up a four-connected uninodal 3D supramolecular net with **dia** topology and (6^6) point symbol that would represent a new porous material with an estimated internal surface area of 3600 m^2/g and 67% of void space.

Nevertheless, it would contain such huge channels that the real crystal structure involves three interpenetrated networks that occupy all the available space providing a nonporous material. This entanglement problem is also common in MOFs.[34] Porous materials try to minimize the system energy through optimal filling of void space, but structural interpenetration may occur only if the pore space of an individual net is sufficiently large to accommodate an additional net. In addition to this, various weak supramolecular forces such as H-bonding, $\pi-\pi$ aromatic stacking interactions, and van der Waals forces are believed to play vital roles in the formation of interpenetrated structures. **SMOF-5** follows the same pattern, provided that it contains such a huge percentage of void. Thus, the resulting structure can be described as a 3-fold interpenetrated network as shown in Figure 4b. The attempt to avoid this interpenetration using the more voluminous bromide anion instead of chloride did not succeed, providing the same triple interpenetrated supramolecular structure (**SMOF-6**, see Supporting Information).

Table 3. Hydrogen Bonding Interactions (Å, °) in SMOF-5[a]

D−H···A[b]	H···A	D···A	D−H···A
N6−H6A···N1^{ii}	2.06	2.912(6)	173
N6−H6B···Cl1^{i}	2.39	3.237(4)	167
N9−H9···N3^{iii}	2.11	2.833(6)	165

[a]Symmetry codes: (i) $-x, y, -z + 1/2$; (ii) $-x + 1/2, -y + 1/2, -z + 1$; (iii) $-x, -y - 1, -z + 1$. [b]D: donor; A: acceptor.

Structural Description of $[Cu_8(\mu_4\text{-}OH)_4(\mu_3\text{-}OH)_4(ade)_4(\mu\text{-}ade)_4(\mu\text{-}Hade)_2]$ (SMOF-7). This compound consists of $[Cu_8(\mu_4\text{-}OH)_4(\mu_3\text{-}OH)_4(\text{adeninato-}\kappa N9)_4(\mu\text{-adeninato-}\kappa N3{:}\kappa N9)_4(\mu\text{-adenine-}\kappa N3{:}\kappa N9)_2]$ octameric clusters formed by the stacking of four $Cu_2(\mu\text{-OH})_2$ dimers that are 90° rotated and linked by a semicoordination to the neighboring Cu(II) atoms through the hydroxide bridges (Figure 5a). The resulting aggregate can be described as the stacking of three cubanes (cubes with the vertices alternatively occupied by the metal and the bridging ligand). The surface of each octamer is occupied by eight adeninate and two neutral adenine ligands. Four adeninato and the neutral adenine entities act as bidentate *N*3,*N*9-bridging ligands. These bridging ligands are disordered into two coplanar arrangements with inverted orientation regarding the coordination mode ($\mu\text{-}\kappa N3{:}\kappa N9/\mu\text{-}\kappa N9{:}\kappa N3$).[35,36] The remaining adeninato ligands are anchored to the corners of the cluster as terminal ligands through N9, and their stiffness is reinforced by intramolecular hydrogen bonds involving the hydroxide bridges and the N3 positions of the nucleobases. All the adenines, adeninates, and hydroxides are rigidly anchored to the octameric entity because of their multiple coordination bond (OH/adenine/adeninato) or the combination of a coordination bond and an intramolecular hydrogen bond (adeninato).

The interaction of each octamer with the adjacent ones is by means of a hydrogen bonding scheme involving the hydroxide anions and the N7 imidazolic atom of terminal adeninato ligands giving rise to a bidimensional network. Moreover, the bridging adeninato ligands direct their Watson−Crick and Hoogsteen faces outward in those supramolecular layers in such a way that they establish complementary hydrogen bonding interactions with neighboring tectons. As in previous compounds the Watson−Crick faces establish a $R_2^2(8)$ hydrogen bonding ring. The combination of the above-described interactions leads to a 3D 8c uninodal supramolecular net with a **sqc3** topology, point symbol being ($4^4.6^2$), where the geometrical requirements imposed by the rigidity of the octameric unit and the hydrogen bonding interactions avoid the full occupancy of the space. This is reflected by the presence of large monodimensional channels of ca. 4.9 Å

DOI: 10.1021/cg501804h
Cryst. Growth Des. 2015, 15, 975−983

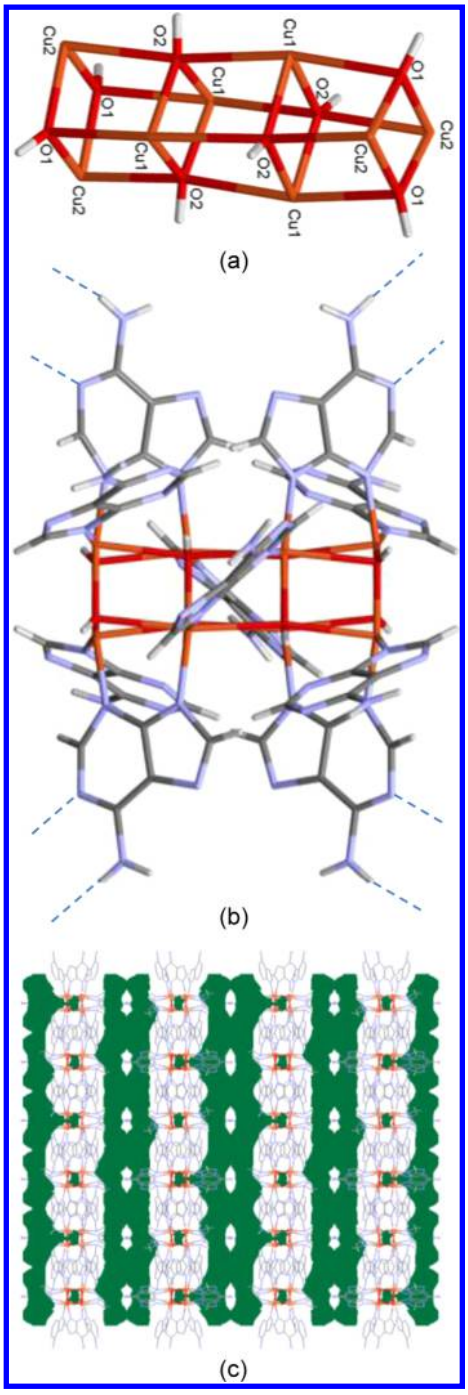

Figure 5. (a) $[Cu_8(\mu_4\text{-}OH)_4(\mu_3\text{-}OH)_4]$ unit, (b) whole octameric entity, and (c) three-dimensional packing of **SMOF-7**.

spreading along the [100] direction, which corresponds to a calculated surface area of 366 m^2/g and a 30% of void space.

Structural Description of $[Cu_4(\mu_3\text{-ade})_4(\mu\text{-ade})_2(pentylNH_2)_2(CH_3OH)_2(CO_3)_2(H_2O)_2]\cdot n$(solvent) (SMOF-8). **SMOF-8** is built up by tetranuclear $[Cu_4(\mu_3\text{-ade})_2(\mu\text{-ade})_2(pentylNH_2)_2(CH_3OH)_2(CO_3)_2(H_2O)_2]$ units in which two types of neutral building units coexist: a dimeric $[Cu_2(\mu\text{-ade})_4(H_2O)_2]$ entity and two monomeric $[Cu(pentylNH_2)(CH_3OH)(CO_3)]$ moieties (Figure 6).

The dimeric fragment is centrosymmetric and is made of two Cu(II) atoms bridged by four μ-*N*3,*N*9-adeninate anions in a paddle-wheel shaped arrangement. The apical position of the

Table 4. Hydrogen Bonding Interactions (Å, °) in SMOF-7[a]

D−H···A[b]	H···A	D···A	D−H···A
N16−H16A···N11A[iii]	2.51	3.34(3)	161
N36−H36B···N13[i]	2.56	3.317(7)	148
O1−H1···N37[iv]	2.09	2.947(5)	177
O2−H2···N33[v]	2.18	3.015(6)	167

[a]Symmetry codes: (i) $x, -y + 1/2, -z + 1/2$; (iii) $-x + 3/2, y, z - 1/2$; (iv) $-x + 3/2, -y + 1, z$; (v) $-x + 3/2, y, z + 1/2$. [b]D: donor; A: acceptor.

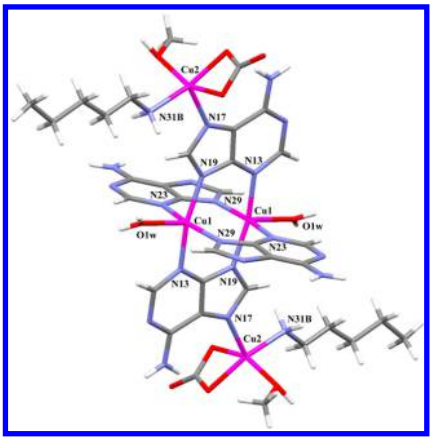

Figure 6. Structural unit of **SMOF-8** with the atomic numbering scheme.

distorted square pyramidal coordination around Cu1 atom is completed with a water molecule. Each dimeric entity is linked to two neighboring monomeric units via the N7 imidazolic atoms of two adeninato ligands. Therefore, two adeninate anions behave as tridentate μ_3-*N*3,*N*7,*N*9 bridging ligands, whereas the other two act as bidentate μ-*N*3,*N*9. The basal plane of the square pyramidal chromophore around Cu2 atom is completed with two oxygen atoms from a carbonato ligand, an oxygen atom of a methanol molecule, and the nitrogen atom of a pentylamine molecule.

Each tetranuclear entity is linked to four adjacent ones via double N6−H···N1 hydrogen bonding interactions between the Watson−Crick faces of neighboring entities to give a $R_2^2(8)$ ring. This assembling of tetrameric entities gives rise to layers that can be described as a four-connected uninodal net with Shubnikov tetragonal **sql** topology and $(4^4.6^2)$ point symbol. It is worth noting that the dinuclear paddle-wheel entity of **SMOF-1** and **SMOF-2** presents analogous four-connected nodes (using Watson−Crick base pairing interactions), but the absence of the bulky capping monomeric entities allows the growth of a 3D supramolecular network (**nbo**, $6^4.8^2$). However, in **SMOF-8** the 3D cohesion requires additional hydrogen bonding interactions involving the coordination water molecule, the carbonato ligand, and the pentylamine molecule (Figure 7, Table S4) leading to an α-Po **pcu** topology. The overall packing generates a 2D pore network with channels running along the *b* and *c* axes of 3−5 Å of diameter, that represents 43% of void space and a calculated surface area of 402 m^2/g. However, the crystals decompose upon removal from the mother liquor and even when immersed in pure methanol. This fact is probably due to the loss of pentylamine that seems to play a key role stabilizing the crystal structure.

Structural Description of $[Cu_2(\mu\text{-ade})_2(ade)(\mu\text{-OH})(H_2O)(CH_3OH)]_n\cdot n$(solvent) (SMOF-9). The basic structural

DOI: 10.1021/cg501804h
Cryst. Growth Des. 2015, 15, 975−983

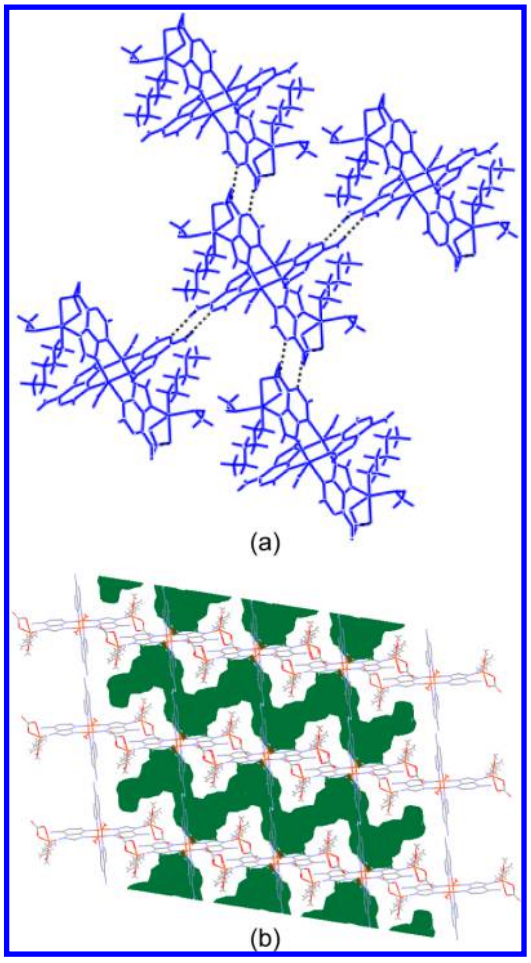

Figure 7. (a) Linkage of the tetranuclear entities by the Watson−Crick faces and (b) crystal packing along the *b* axis of **SMOF-8**, showing the generated voids.

Table 5. Hydrogen Bonding Interactions (Å, °) in SMOF-8[a]

D−H···A[b]	H···A	D···A	D−H···A
N6−H6A···N11[ii]	2.13	2.978(11)	167
N6−H6B···O1	2.11	2.965(13)	175
N6−H26B···N21[iii]	2.08	2.935(17)	172
O1w−H12w···O3[iv]	1.94	2.790(13)	169
N31−H31A···O2[v]	1.94	2.843(18)	176

[a]Symmetry codes: (ii) $-x + 2, -y + 1, -z + 1$; (iii) $-x + 2, -y, -z$; (iv) $x - 1, y, z$; (v) $-x + 3, -y, -z + 1$. [b]D: donor; A: acceptor.

unit of this compound consists of 1D infinite coordination polymers held together by complementary hydrogen bonding interactions in a 3D supramolecular porous structure. The coordination polymer can be described as noncentrosymmetric dinuclear units (Figure 8) in which two Cu(II) atoms are bridged with two adeninate moieties by the N3 and N9 atoms and also by one hydroxyl group (Figure 9a). One of the metal centers is also coordinated to a water molecule while the other to the oxygen atom of a methanol molecule. These dinuclear units are connected by additional bridging adeninates that are coordinated to the Cu(II) centers by the N7 and N9 atoms to provide a 1D coordination chain. An interesting structural feature is that the bridging adeninates inside the dinuclear units are tilted by 22°, but they present wider tilt angle with respect to those connecting the dimeric units (56 and 78°, respectively)

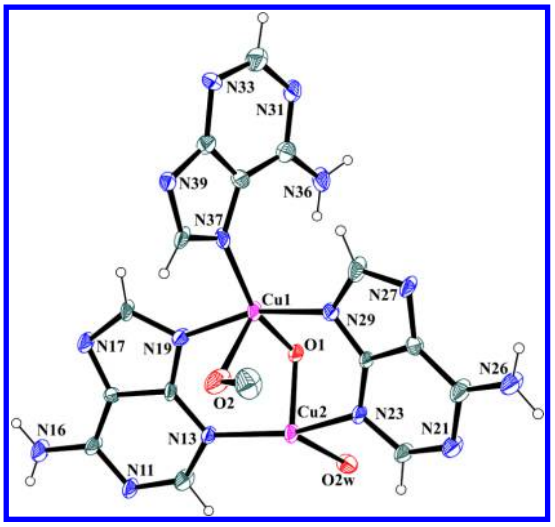

Figure 8. Ortep representation of the dimeric unit $[Cu_2(\mu\text{-ade})_2(ade)(H_2O)(\mu\text{-OH})(CH_3OH)]$ together with the numbering scheme in **SMOF-9**.

in the polymeric chain. This fact together with the complementary double hydrogen bonding interactions of the nucleobases promotes a three-dimensional propagation of the supramolecular structure. The μ-$\kappa N3$:$\kappa N9$-adeninates are able to establish double WC···WC and H···H synthons leading to $R_2^2(8)$ and $R_2^2(10)$ hydrogen bonding rings, respectively. On the other hand, the μ-$\kappa N7$:$\kappa N9$-adeninates are hydrogen bonded to the bridging hydroxide and the coordinated water molecule of an adjacent polymeric chain through N1 and N6 positions of the Watson−Crick face. The resulting supramolecular crystal structure shows the presence of large channels along the *b* axis with a calculated surface area of 295 m^2/g and 44% of void space.

This compound is an interesting case because it is in between pure MOFs and SMOFs as it polymerizes into 1D through coordination bonds and further extends to supramolecular array through complementary hydrogen bonding interactions resulting in a 3D porous network (Figure 9c).

CONCLUSIONS

In this report we have paid special attention to the design prerequisites of SMOFs: (i) rigid building unit/complex, (ii) rigid and predictable synthons, and (iii) at least three noncoplanar synthons. This approach is supported by six new SMOFs based on different metal centers, nucleobases, and synthetic conditions. It also highlights the suitability of metal-nucleobase systems, specially purine based ones, to obtain SMOFs since many of them accomplish the above stated requirements: (i) the rigidity of the building unit is achieved using nucleobases because they can be coordinated through multiple positions, normally by a double anchoring (double coordination bonds or the combination of a coordination bond and an intramolecular hydrogen bond), (ii) the well-known complementary hydrogen bonding interactions between the nucleobases ensures the necessary rigidity of the predictable synthons, and (iii) the metal coordination geometries impose, in many cases, a non-coplanar arrangement of the nucleobases affording a non-coplanar disposition of the synthons that allows three-dimensional propagation of the nucleobase···nucleobase complementary hydrogen bonding assembly.

DOI: 10.1021/cg501804h
Cryst. Growth Des. 2015, 15, 975−983

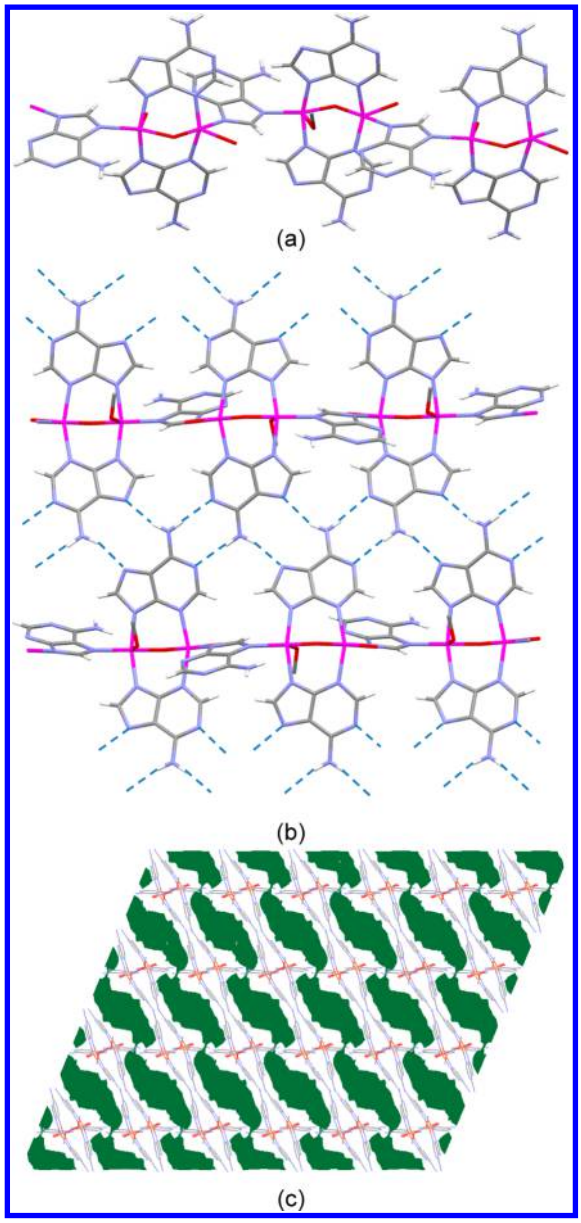

Figure 9. (a) Coordination polymeric chain. (b) Supramolecular complementary base pairing interactions among the adeninate entities. (c) Porous supramolecular architecture of **SMOF-9** along the *b* axis.

Table 6. Hydrogen Bonding Interactions (Å, °) in SMOF-9[a]

D−H···A[b]	H···A	D···A	D−H···A
N16−H16A···N11^{ii}	2.23	3.075(10)	170
N26−H26A···N21^{iii}	2.06	2.920(11)	179
N26−H26B···N17^{iv}	2.08	2.904(11)	161
N36−H36B···O1^{v}	2.12	2.884(9)	148

[a]Symmetry codes: (ii) $-x + 1, -y + 2, -z + 1$; (iii) $-x, -y + 2, -z$; (iv) $x - 1/2, -y + 3/2, z - 1/2$; (v) $-x + 1/2, -y + 3/2, -z$. [b]D: donor; A: acceptor.

■ ASSOCIATED CONTENT

Supporting Information

Tables of coordination bond lengths, figures of network topologies, XRPD patterns, and cif files. This material is available free of charge via the Internet at http://pubs.acs.org.

■ AUTHOR INFORMATION

Corresponding Authors

*(O.C.) E-mail: oscar.castillo@ehu.es. Fax: (internat): +34 946013500.

*(S.P.-Y.) E-mail: sonia.perez@ehu.es.

Author Contributions

‡These authors (J.T.-G and R.P.-A) contributed equally.

Notes

The authors declare no competing financial interest.

■ ACKNOWLEDGMENTS

This work has been funded by Ministerio de Economía y Competitividad (MAT2013-46502-C2-1-P), Eusko Jaurlaritza/Gobierno Vasco (Grant IT477-10, S-PE13UN016), and Universidad del País Vasco/Euskal Herriko Unibertsitatea (EHUA14/09, UFI 11/53, postdoctoral fellowship for S.P.Y.). Technical and human support provided by SGIKer (UPV/EHU, MINECO, GV/EJ, ERDF, and ESF) is gratefully acknowledged.

■ REFERENCES

(1) Zhou, H.-C.; Long, J. R.; Yaghi, O. M. *Chem. Rev.* **2012**, *112*, 673.
(2) Seo, J.; Jin, N.; Chun, H. *Inorg. Chem.* **2010**, *49*, 10833.
(3) Bae, Y. S.; Farha, O. K.; Hupp, J. T.; Snurr, R. Q. *J. Mater. Chem.* **2009**, *19*, 2131.
(4) Simard, M.; Su, D.; Wuest, J. D. *J. Am. Chem. Soc.* **1991**, *113*, 4696.
(5) Kim, H.; Kim, Y.; Yoon, M.; Lim, S.; Park, S. M.; Seo, G.; Kim, K. *J. Am. Chem. Soc.* **2010**, *132*, 12200.
(6) Holden, A. *Shapes, Space, and Symmetry*; Dover: New York, 1991; pp 154−163.
(7) Thomas-Gipson, J.; Beobide, G.; Castillo, O.; Fröba, M.; Hoffmann, F.; Luque, A.; Pérez-Yáñez, S.; Román, P. *Cryst. Growth Des.* **2014**, *14*, 4019.
(8) Reger, D. L.; Debreczeni, A.; Smith, M. D.; Jezierska, J.; Ozarowski, A. *Inorg. Chem.* **2012**, *51*, 1068.
(9) Beobide, G.; Castillo, O.; Cepeda, J.; Luque, A.; Pérez-Yáñez, S.; Román, P.; Thomas-Gipson, J. *Coord. Chem. Rev.* **2013**, *257*, 2716.
(10) Stylianou, K. C.; Warren, J. E.; Chong, S. Y.; Rabone, J.; Bacsa, J.; Bradshaw, D.; Rosseinsky, M. J. *Chem. Commun.* **2011**, *47*, 3389.
(11) Kundu, S.; Mohapatra, B.; Mohapatra, C.; Verma, S.; Chandrasekhar, V. *Cryst. Growth Des.* **2015**, *15*, 247.
(12) Thomas-Gipson, J.; Beobide, G.; Castillo, O.; Cepeda, J.; Luque, A.; Pérez-Yáñez, S.; Aguayo, A. T.; Román, P. *CrystEngComm* **2011**, *13*, 3301.
(13) Nugent, P. S.; Rhodus, V. L.; Pham, T.; Forrest, K.; Wotjas, L.; Space, B.; Zaworotko, M. J. *J. Am. Chem. Soc.* **2013**, *135*, 10950.
(14) *CrysAlis RED*, version 1.171.33.55; Oxford Diffraction: Wroclaw, Poland, 2010.
(15) Altomare, A.; Cascarano, M.; Giacovazzo, C.; Guagliardi, A. *J. Appl. Crystallogr.* **1993**, *26*, 343.
(16) Sheldrick, G. M. *SHELXL-97, Program for X-ray Crystal Structure Refinement*; University of Göttingen: Göttingen, Germany, 1997.
(17) Farrugia, L. J. *J. Appl. Crystallogr.* **1999**, *32*, 837.
(18) Van der Sluis, P.; Spek, A. L. *Acta Crystallogr.* **1990**, *A46*, 194.
(19) Spek, A. L. *J. Appl. Crystallogr.* **2003**, *36*, 7.
(20) Amo-Ochoa, P.; Alexandre, S. S.; Hribesh, S.; Galindo, M. A.; Castillo, O.; Gómez-García, C. J.; Pike, A. R.; Soler, J. M.; Houlton, A.; Zamora, F. *Inorg. Chem.* **2013**, *52*, 5290.
(21) García-Couceiro, U.; Castillo, O.; Cepeda, J.; Lanchas, M.; Luque, A.; Pérez-Yáñez, S.; Román, P.; Vallejo-Sánchez, D. *Inorg. Chem.* **2010**, *49*, 11346.
(22) Coronado, E.; Galán-Mascarós, J. R.; Gómez-García, C. J.; Laukhin, V. *Nature* **2000**, *408*, 447.
(23) TOPOS Main Page. http://www.topos.ssu.samara.ru (accessed Apr. 2014).

DOI: 10.1021/cg501804h
Cryst. Growth Des. 2015, 15, 975−983

(24) Blatov, V. A. *IUCR CompComm Newsletter* **2006**, *7*, 4.
(25) O'Keeffe, M.; Yaghi, O. M. *Chem. Rev.* **2012**, *112*, 675.
(26) Sarkisov, L.; Harrison, A. *Moleular Simulation* **2011**, *37*, 1248.
(27) Pérez-Yáñez, S.; Beobide, G.; Castillo, O.; Cepeda, J.; Luque, A.; Román, P. *Cryst. Growth Des.* **2012**, *12*, 3324.
(28) Pandey, M. D.; Mishra, A. K.; Chandrasekhar, V.; Verma, S. *Inorg. Chem.* **2010**, *49*, 2020.
(29) Mishra, A. K.; Purohit, C. S.; Kumar, J.; Verma, S. *Inorg. Chim. Acta* **2009**, *362*, 855.
(30) Beck, W. M.; Calabrese, J. C.; Kottmair, N. D. *Inorg. Chem.* **1979**, *18*, 176.
(31) Sánchez-Moreno, M. J.; Choquesillo-Lazarte, D.; González-Pérez, J. M.; Carballo, R.; Castiñeiras, A.; Niclós-Gutiérrez, J. *Inorg. Chem. Commun.* **2002**, *5*, 800.
(32) Pérez-Yáñez, S.; Castillo, O.; Cepeda, J.; García-Terán, J. P.; Luque, A.; Román, P. *Inorg. Chim. Acta* **2011**, *365*, 211.
(33) An, J.; Fiorella, R. P.; Geib, S. J.; Rosi, N. L. *J. Am. Chem. Soc.* **2009**, *131*, 8401.
(34) Shekhah, O.; Wang, H.; Paradinas, M.; Ocal, M.; Schüpbach, B.; Terfort, A.; Zacher, D.; Fischer, R. A.; Wöll, C. *Nat. Mater.* **2009**, *8*, 481.
(35) Cepeda, J.; Castillo, O.; García-Terán, J. P.; Luque, A.; Pérez-Yáñez, S.; Román, P. *Eur. J. Inorg. Chem.* **2009**, 2344.
(36) Pérez-Yáñez, S.; Beobide, G.; Castillo, O.; Cepeda, J.; Luque, A.; Román, P. *Cryst. Growth Des.* **2013**, *13*, 3057.

DOI: 10.1021/cg501804h
Cryst. Growth Des. 2015, 15, 975−983